MALAYSIAN JOURNAL OF SCIENCE
MJS
ISSN 1394 - 3065

2nd Euro-Asia Conference on CO_2 Capture and Utilization (EACCO2CU2022) Special Issue

Malaysian Journal of Science 43 (Special Issue 1): 58-66 (July 2024) https://mjs.um.edu.my

INVESTIGATION OF CARBON DIOXIDE ABSORPTION CAPACITY AND DISSOLUTION RATE WITH AMINO ACID SALT SOLUTIONS: SODIUM AND POTASSIUM GLYCINATE

İrem Koçyiğit Çapoğlu[1a], Duygu Uysal[2b*] and Özkan Murat Doğan[3c]

Abstract: Global warming is a major world problem and causes climate change. The primary cause of global warming is carbon dioxide (CO_2) emissions. Ongoing studies are being conducted to mitigate the effects of this problem. Anthropogenic CO_2 emissions occur by burning fossil fuels to generate power and heat. To combat this problem, CO_2 must be captured from point emission sources or directly from air. The conventional method to remove CO_2 at the point emission sources is post-combustion systems. In these systems, absorption process is generally used to diminish CO_2 emission and capturing at the source. Current researches aim to find an efficient and alternative solution to absorption. In this work, sodium glycinate (NaGly) and potassium glycinate (KGly), which are amino acid salt solutions, were investigated for CO2 absorption. Amino acid salt solutions have shown similar absorption kinetics and capacities to amine-based solutions due to same functional group. These solutions are usually more stable to oxidative degradation and have low volatilities, higher surface tensions and the viscosities are very close to waters. Experiments were performed using a stirred cell system at ambient temperature (20°C) and atmospheric pressure (91 kPa), in Ankara, Türkiye. In experiments, sodium glycinate and potassium glycinate concentration was ranged between 0.1 and 1.5 M. The experiments were also repeated with sodium hydroxide and potassium hydroxide in the same concentration range for comparison. In addition, the amino acid salt solutions examined in this study were compared with alkaline solutions and glycine in terms of total CO_2 absorption capacity and CO_2 dissolution rate. As a result of the experiments, the potassium glycinate solutions gave approximately 1.4 times better results than the sodium glycinate solutions at the highest concentration. Also, functional groups were determined by FTIR analysis of pure and CO_2-loaded potassium glycinate solution.

Keywords: carbon dioxide, absorption, amino acid, sodium glycinate, potassium glycinate.

1. Introduction

Carbon dioxide (CO_2) emissions rapidly increase worldwide, most of which stem from anthropogenic activities. The latest atmospheric CO_2 concentration reached 421 ppm in May 2023 and this trend unfortunately continuously increasing (NASA, 2023). According to the Intergovernmental Panel on Climate Change (IPCC), CO_2 emissions must reach net zero by 2050 with no or limited temperature rise (IPCC, 2022). Using fossil fuels in combustion processes with increasing energy demand is directly associated with excessive CO_2 concentrations in the atmosphere. Humanity's main energy source is still fossil fuels, and CO_2 must be captured from the atmosphere or point emission sources (such as power plants) to reduce emissions (Yuan et al., 2022; Keith et al., 2018). Carbon dioxide capture and storage (CCS) or carbon dioxide capture and utilization (CCU) technologies are considered to have significant potential for decarbonization (Zhang & Huisingh, 2017). To capture CO_2 there are three systems recommended mainly: pre-combustion, post-combustion, and oxy-fuel combustion. (Buckingham et al., 2022; Ahmed et al., 2020). The gas streams' pressure, CO_2 concentration, and fuel type (e.g., coal or natural gas) are considerable factors in choosing the capture system (Olajire, 2010).

In post-combustion capture systems, CO_2 is captured from flue gases produced because of the combustion of fuels with high carbon sources such as fossil fuels and biomass. Post-combustion systems use a liquid solution to capture the small fraction of CO_2 (typically 3–15% by volume) present in a flue gas stream (IPCC, 2005). Post-combustion carbon capture has important potential because it can be retrofitted to existing units in the power sector. Currently, conventional pulverized coal (PC) power plants or natural gas combined cycle (NGCC) power plants use post-combustion capture systems that employ an organic solution such as monoethanolamine (MEA) (Figueroa et al., 2008).

There are many methods for capturing CO_2. Common methods for CO_2 capture are absorption, adsorption, separation with a membrane, cryogenic separation, etc. (Wu et al., 2020). Among all these systems and methods, the most used system is the post-combustion/absorption mechanism because of reliable technology, large operation capacity, and longtime industrial process experience (Wang et al., 2011; Ochedi et al., 2021). CO_2 absorption with the solution can occur in two ways: physical or chemical absorption. There are several CO_2 capture solutions available including, alkanolamine solutions (Murrieta-Guevara et

Authors information:
[a]Graduate School of Natural and Applied Sciences, Main Campus, Gazi University, 06500, Ankara, Türkiye, E-mail: iremkocyigit@gazi.edu.tr[1]
[b]Chemical Engineering Department, Gazi University, Faculty of Engineering, Maltepe, Ankara, 06570, Türkiye, E-mail: duysal@gazi.edu.tr[2]
[c]Chemical Engineering Department, Gazi University, Faculty of Engineering, Maltepe, Ankara, 06570, Türkiye, E-mail: mdogan@gazi.edu.tr[3]

*Corresponding Author: duysal@gazi.edu.tr

Received: February 7, 2024
Accepted: May 7, 2024
Published: July 31, 2024

DOI: https://doi.org/10.22452/mjs.vol43sp1.10
Malaysian Journal of Science 43 (Special Issue 1): 58-66 (July 2024)

al., 1988; Puxty et al., 2009; Bernhardsen & Knuutila, 2017), ionic liquids (ILs) (Babamohammadi et al., 2015), liquid ammonia (Wang et al., 2018), polyethylene glycol (Li et al., 2012), methanol (Gatti et al., 2014), potassium carbonate (Ghosh et al., 2009), and others. Alkanolamine solutions such as monoethanolamine (MEA), diethanolamine (DEA), and methyl diethanolamine (MDEA) are mostly used as an absorbent in commercial applications (Aghel et al., 2021). However, these solutions have several drawbacks related to limited cyclic carbon dioxide loading capacity, degradation by oxygen, high equipment corrosion and the operating cost is fairly high due to the high energy requirement for regeneration of the solution (Ahn et al., 2010; Luis, 2016). Therefore, studies on CO_2 absorption have focused on finding efficient, environmentally friendly energy-saving alternative solutions that may eliminate the disadvantages of the current systems.

Recently, it has been seen that amino acid salts have shown significant potential in CO_2 absorption. The latest research shows that amino acid salts could be replaced with alkanolamine solutions due to their molecular structure similarity (Kumar et al., 2003; Harris et al., 2009). Amino acid salts are formed by equimolar mixing an alkaline solution with amino acids such as glycine and sarcosine (Lee et al., 2007). Amino acid salt solutions have certain advantages over amines such as higher surface tension, low volatility, low toxicity, high biodegradation potential, resistance to oxidative degradation, and better absorption capacity (Guo et al., 2013; Majchrowicz et al., 2014; Hu et al., 2018). Because of these substantial properties, amino acid salt solutions have been used commercially as the promoters in carbonate solutions in the Giammarco-Vetrocoke process (Thee et al., 2013), selective acid gas removal from industrial gas streams in the Alkacid process by BASF (Vaidya et al., 2010), as precipitating solutions in the DECAB process (Fernandez & Goetheer, 2011), and in post-combustion CO_2 capture in the Siemens POSTCAP process (Majchrowicz et al., 2014).

The absorption of monoethanolamine (MEA) and amino acid salt solutions with carbon dioxide is chemical absorption. Similar to primary and secondary amines, since it has the same functional groups (amine groups), CO_2 is expected to react with the amino acid salt solution via the zwitterionic mechanism (Kumar et al., 2003; Lee et al., 2007). The zwitterion mechanism was first introduced by Caplow (1968) and later explained by Danckwerts (1979). The general reactions occurring during amine-CO_2 absorption can be summarized as carbamate formation, bicarbonate formation, and carbonic acid formation.

In amine-CO_2 absorption, first the free electrons in the nitrogen atom attack the carbon atom in the CO_2 and form the zwitterion. The zwitterion formation reaction is shown by Eq. (1) (Caplow, 1968; Kumar et al., 2003; Lee et al., 2007).

$$CO_2 + RNH_2 \underset{k_{-1}}{\overset{k_2}{\rightleftarrows}} RNH_2^+COO^- \quad (1)$$

Considering MEA, the R expression can be expressed as: $R = HOCH_2CH_2-$. Subsequently, it gives the zwitterion proton to a free base, forming carbamate (carbamic acid). The proton transfer to the free base B is shown by Eq. (2). In this reaction, the proton transfer reaction can be considered irreversible as the equilibrium predominates on the right side of the reaction (Majchrowicz et al., 2014).

$$RNH_2^+COO^- + B \overset{k_B}{\rightarrow} RNHCOO^- + BH^+ \quad (2)$$

The base referred to herein as B may be any of the amine, water, or hydroxyl (OH^-) groups. The contribution of these groups during proton transfer is shown by Eq. (3), Eq. (4), and Eq. (5) (Lee et al., 2007)

$$RNH_2^+COO^- + H_2O \rightarrow RNHCOO^- + RNH_3^+ \quad (3)$$

$$RNH_2^+COO^- + RNH_2 \rightarrow RNHCOO^- + H_3O^- \quad (4)$$

$$RNH_2^+COO^- + OH^- \rightarrow RNHCOO^- + H_2O \quad (5)$$

During the formation of zwitterion, the reaction of carbon dioxide with hydroxyl ions in the water also occurs simultaneously, albeit in small amounts, and bicarbonate ions are formed. The reactions are shown by Eq. (6) and Eq. (7).

$$H_2O \rightleftarrows H^+ + OH^- \quad (6)$$

$$CO_2 + OH^- \rightleftarrows HCO_3^- \quad (7)$$

The carbonic acid formation reaction is quite slow and negligible (Lee et al., 2007). The reaction is shown by Eq. (8).

$$CO_2 + H_2O \rightleftarrows HCO_3^- + H^+ \quad (8)$$

The reaction rate of the quasi-steady state between CO_2 and amino acids for the zwitterionic mechanism (considering all possible free bases-$\sum k_b\,[B]$) can be described as follow:

$$r_{CO_2,abs} = \frac{k_2\,[CO_2][Am]}{1+\frac{k_{-1}}{k_b\,[B]}} \quad \frac{[CO_2][RNH]}{\frac{1}{k_2}+\frac{k_{-1}}{k_2}\frac{1}{\sum k_b\,[B]}} = k_{app}\,[CO_2] \quad (9)$$

Here, k_{app} is called the apparent rate constant. If the deprotonation of the zwitterion is much faster than the reverse rate of the first reaction $\left(\frac{k_{-1}}{\sum k_b\,[B]} \ll 1\right)$, the rate of absorption of carbon dioxide is reduced to a simple second-order reaction rate expression. In this case, the reaction rate equation is shown as in Eq. (10).

$$r_{CO_2,abs} = k_2\,[CO_2][RNH] = k_{app}\,[CO_2] \quad (10)$$

While the above expression is accepted as valid for simple amine groups such as MEA, the reaction expression is shown as in Eq. (11) since $\left(\frac{k_{-1}}{\sum k_b\,[B]} \gg 1\right)$ for large volume amine groups.

$$r_{CO_2,abs} = k_2\,[CO_2][RNH]\left(1+\frac{\sum k_b\,[B]}{k_{-1}}\right) \cong k_2\,[CO_2][RNH]\left(\frac{\sum k_b\,[B]}{k_{-1}}\right) = k_{app}\,[CO_2] \quad (11)$$

Considering the reaction of CO_2 directly with hydroxyl ions in water, the total rate constant and reaction rate expression can be written as Eq. (12) and Eq. (13).

$$k_{ov} = k_{app} + k_{OH^-}[OH^-] \quad (12)$$

$$r_{CO_2,abs} = k_{ov}\,[CO_2] \quad (13)$$

This work focuses on the determination of the total CO_2 absorption capacity and dissolution rate of the amino acid salt solutions potassium glycinate (KGly) and sodium glycinate (NaGly) and their comparison with alkaline solutions sodium hydroxide

DOI: https://doi.org/10.22452/mjs.vol43sp1.10
Malaysian Journal of Science 43 (Special Issue 1): 58-66 (July 2024)

(NaOH) and potassium hydroxide (KOH). All experiments were carried out in a stirred cell at ambient temperature (20°C) and atmospheric pressure (91 kPa). pH measurements of the solutions were made before and after CO_2 absorption. The solution concentration varied between 0.1 to 1.5 M. In addition, amino acid functional groups were determined by FTIR analysis of potassium glycinate solution. FTIR analysis was applied to both pure potassium glycinate solution and CO_2-loaded potassium glycinate solution, and the results are presented in this study.

2. Materials and methods

2.1 Materials

The CO_2 gas cylinder (>99.99%) was supplied from Samtaş A.Ş. Glycine were purchased from Carlo Erba and, sodium hydroxide (NaOH) and potassium hyrdroxide (KOH) pellets were purchased from Merck. Aqueous sodium glycinate and potassium glycinate solutions were prepared by neutralizing glycine dissolved in distilled water, with equimolar sodium hydroxide and potassium hydroxide, respectively. The measurements of weight were employed using an analytical balance with an ±0.1 mg accuracy. During the experiments, the absorption solution was stirred with a VELP SCIENTIFICA ARE model magnetic stirrer. The pressure drop in the system was measured with HK Instruments DPT-R8 model pressure transmitter and recorded on the computer with the ORDEL UDL100 model data logger. In all experiments, pH measurements were made with a WTW pH 3110 model pH meter.

2.2 Experimental Set-Up

Experiments were carried out in stirred cell reactor. Stirred cell reactor is a known equipment for employed reaction and mass transfer studies in gas-liquid systems (Kucka et al., 2003; Ying & Eimer 2013). Stirred cell reactor experiment principle is based on the gas in the gas chamber being absorbed into the liquid in time. By observing the pressure drop in the gas chamber along with the amount of gas absorbed into the liquid, it is possible to calculate how much gas is absorbed. The schematic experimental set-up is shown in Fig. (1).

The stirred cell reactor system consists of two parts, a 0.5 L gas chamber and a 0.4 L liquid reservoir. The reactor part is made of pyrex glass. The gas chamber has valves to which the gas inlet and outlet are connected. A CO_2 gas cylinder is attached to the gas chamber. Before the gas was fed to the system, it was passed through the humidifier to keep the temperature constant at the gas-liquid interface. Absorption liquid is placed in the liquid reservoir. Two parts of the system are connected by a metal clamp to seal the system.

2.3 Experimental Procedure

In the experiments, firstly, pure CO_2 gas flow is fed to the reactor from the gas inlet, and the air inside the system was swept. Afterward, all valves are closed simultaneously, and CO_2 gas is trapped in the gas chamber. Then, trapped CO_2 gas in the system is absorbed into the absorption solution. As CO_2 is absorbed by the solution, the pressure inside the gas chamber decreased until the constant value is reached. Meanwhile, the absorption solution is stirred with a magnetic stirrer regarding no vibration/vortex forms at the interface.

Through this stirring, mass transfer resistances that may occur on the liquid surface and in the areas close to the surface are prevented by providing homogeneity in the liquid. Also, the solution temperature is instantaneously controlled by a thermocouple with ± 0.2 K accuracies. In the experiments, the pressure drop occurring in the gas chamber is instantly recorded every second on the computer with a data logger using a differential pressure transmitter. While the pressure drop values occurring in the stirred cell reactor were increased at the beginning over time, they were fixed after a while. Then, the total CO_2 absorption capacity and dissolution rate were calculated using the recorded values.

In the experiments glycine, sodium hydroxide, potassium hydroxide, sodium glycinate, and potassium glycinate were used as absorbents with a molar range of 0.1-1.5 M. All experiments were conducted at an ambient temperature of 20°C and an atmospheric pressure of 91 kPa, in Ankara, Türkiye. In all experiments, pH measurements of solutions were made with a pH meter before and after the experiment.

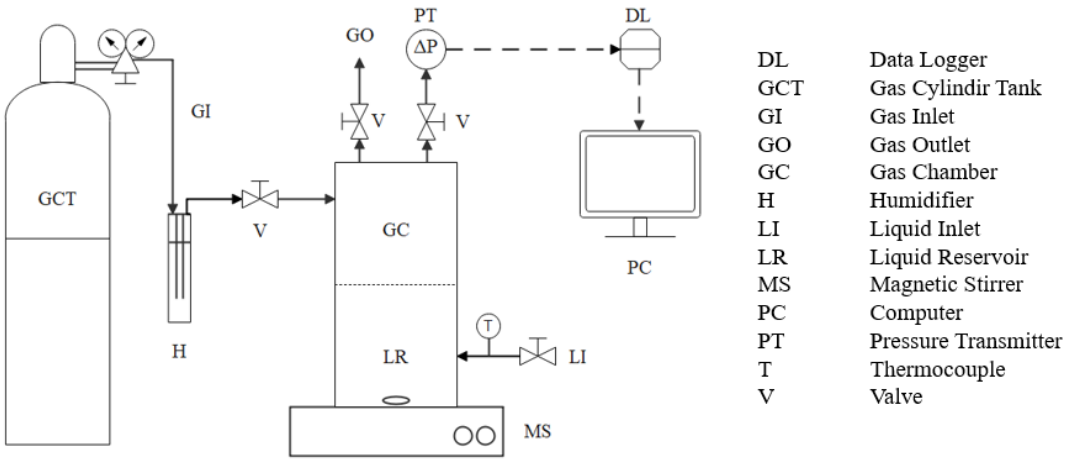

Figure 1. The stirred cell reactor system.

DOI: https://doi.org/10.22452/mjs.vol43sp1.10
Malaysian Journal of Science 43 (Special Issue 1): 58-66 (July 2024)

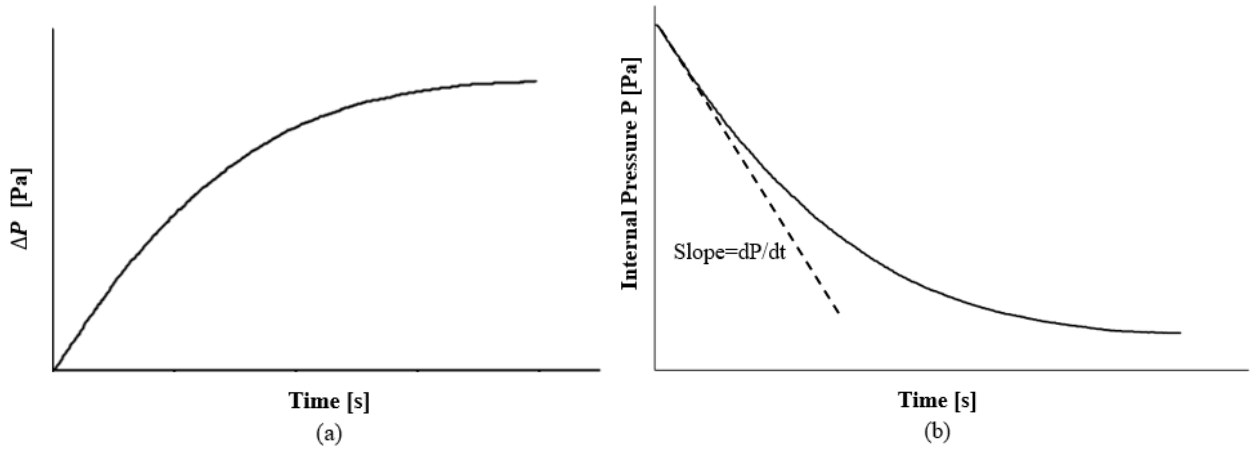

Figure 2. (a) Increase in pressure drop (ΔP) in the gas chamber of the stirred cell reactor with time; (b) The change in the internal pressure (P) in the gas chamber of the stirred cell reactor with time.

2.4 Determination of the Total CO_2 Absorption Capacity

The total CO_2 absorption capacity calculations are made with the ideal gas equation shown in Eq. (14) (Smith et al., 2022).

$$PV_g = ZnRT \quad (14)$$

In this equation, P is the gas pressure [Pa] in the stirred cell reactor gas chamber; V_g is the gas volume [m^3], Z is the compressibility factor [0.995], n is the mole of carbon dioxide gas [mol], R is the gas constant [8.314 Pa-m^3-mol^{-1}-K^{-1}], T is the temperature [K].

The pressure determination in the gas chamber of the stirred cell reactor is calculated with the difference between the atmospheric pressure and the pressure drop measured from the transmitter which is shown in Eq. (15).

$$P = P_{atm} - \Delta P \quad (15)$$

The pressure drop values in the gas chamber were recorded on the computer via the pressure transmitter and then these data were plotted against the time. An example of the graph of the pressure drop versus time in stirred cell reactor is shown in Figure 2 (a). The ordinate of the graph represents the pressure drop difference (ΔP) measured from the transmitter in Pa units, and the abscissa represents the time in seconds.

According to the pressure drop values fixed at the end of the experiment, the mole of CO_2 gas remaining in the gas chamber was calculated with the ideal gas equation (Eq. (14)). Then, by taking the difference between gas moles in the initial and final state, the amount of CO_2 absorbed into the unit volume of absorption liquid also was calculated (Genç Çelikçi, 2020).

2.5 Determination of the Dissolution Rate

The dissolution rate experimental procedure is the same as the total CO_2 absorption capacity experiments but theoretically different. Eq. (16) is obtained by taking and arranging the differential of the ideal gas equation represented by Eq. (14) (Uysal, 2016).

$$dn = \frac{V_g}{ZRT} dP \quad (16)$$

Since the experiments are performed as a function of time, the variation of the expression obtained by Equation 16 with time is shown in Eq. (17) (Uysal, 2016).

$$w = \frac{dn}{dt} = \frac{V_g}{zRT}\frac{dP}{dt} \quad (17)$$

Here w is the dissolution rate [mol-s^{-1}] of CO_2 in absorption solutions. The part on the right side of the equation expresses the change in moles of CO_2 due to the absorption of CO_2 in the gas chamber into the absorption solutions over time.

The internal pressure in the gas chamber was calculated with Eq. (15) and the plot is shown in Figure 2 (b). In order to determine the pressure change (dP/dt) over time, the slope of the first part of the graph, in which it proceeds linearly, was calculated.

The absorption takes place in the liquid reservoir volume (V_L), and the dissolution rate of CO_2 in the solution can be shown by Eq. (18) (Uysal, 2016).

$$r = \frac{w}{V_L} = -\frac{1}{V_L}\frac{V_g}{zRT}\frac{dP}{dt} \quad (18)$$

In Eq. (18), r is the rate of the absorption process relative to the total solution volume from the unit [mol-m^{-3}-s^{-1}], the slope read from the graph from the unit of dP/dt [Pa-s^{-1}] on the right side of the equation, V_L, solution volume [m^3], V_g, gas volume [m^3], T is the gas constant in [K], temperature, R [8.314 Pa-m^3-mol^{-1}-K^{-1}].

3. Results and discussion

3.1. Total CO_2 Absorption Capacity and Dissolution Rate

As a result of all experiments, the dissolution rate (w), the rate of the absorption process relative to the total liquid volume (r), and the total CO_2 absorption capacity were calculated at 20°C and 91 kPa. All experiments were repeated three times and since the values are close to each other, the average values were determined for each solution. The results of the 0.1-1.5 M alkaline solutions (KOH, NaOH) and amino acids (KGly, NaGly) solutions experiment results are shown in Table 1. It was determined that the dissolution rate (w), the rate of the absorption process

DOI: https://doi.org/10.22452/mjs.vol43sp1.10
Malaysian Journal of Science 43 (Special Issue 1): 58-66 (July 2024)

Table 1. Experimental Results of Total CO2 Absorption Capacity and Dissolution Rate for Each Solution.

Solution	Molarity (M)	w* (mol/s)	r** (mol/m³-s)	Total CO_2 absorption capacity (g/L)
KOH	0.1	2.32×10^{-6}	0.006	0.030
	0.5	1.06×10^{-5}	0.026	0.140
	1	2.14×10^{-5}	0.054	0.371
	1.5	2.95×10^{-5}	0.064	0.558
NaOH	0.1	2.98×10^{-6}	0.007	0.071
	0.5	1.09×10^{-5}	0.028	0.132
	1	2.05×10^{-5}	0.048	0.222
	1.5	3.26×10^{-5}	0.081	0.420
KGly	0.1	2.14×10^{-6}	0.005	0.019
	0.5	5.84×10^{-6}	0.015	0.087
	1	6.64×10^{-6}	0.017	0.117
	1.5	1.19×10^{-5}	0.030	0.183
NaGly	0.1	2.37×10^{-6}	0.006	0.020
	0.5	4.81×10^{-6}	0.012	0.062
	1	6.80×10^{-6}	0.017	0.080
	1.5	1.26×10^{-5}	0.031	0.132
Gly	0.1-1.5	$(8.02\text{-}8.30) \times 10^{-7}$	0.0021-0.0022	0.006

w*: Dissolution rate
r**: The rate of the absorption process relative to the total liquid volume

relative to the total liquid volume (r), and the total CO_2 absorption capacity increase as the solution concentration increases.

The dissolution rate (w), the rate of the absorption process relative to the total liquid volume (r), and the total CO_2 absorption capacity are shown graphically in Fig (3), Fig (4), and Fig (5), respectively.

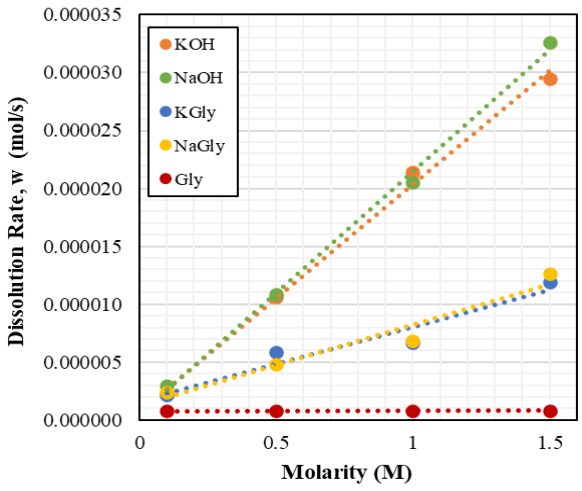

Figure 3. The dissolution rate of CO2 in absorption solutions for comparison of each solution

When the results are compared, alkaline solutions (NaOH and KOH) give better results than amino acid salt solutions (KGly and NaGly), as expected. Because alkaline solutions have high pH so carbonate and bicarbonate formation rates faster than amino acid salt solutions. Also, glycine solution gives the lowest result. Under ambient conditions, potassium glycinate gives slightly better results than sodium glycinate. According to increasing concentration, dissolution rate and total CO_2 absorption capacity

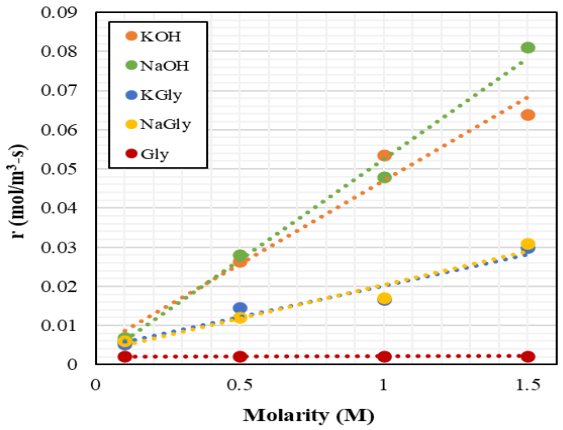

Figure 4. Rate of the absorption process relative to the total liquid volume for comparison of each solution.

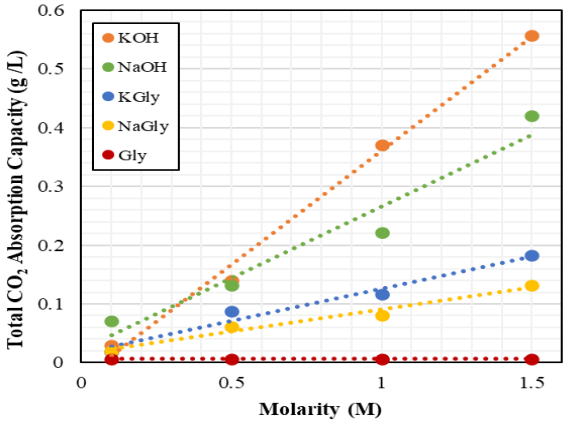

Figure 5. Total CO_2 absorption capacity for comparison of each solution.

DOI: https://doi.org/10.22452/mjs.vol43sp1.10
Malaysian Journal of Science 43 (Special Issue 1): 58-66 (July 2024)

Table 2. Experimental results for total CO_2 absorption capacity of KGly and NaGly

Solution	Concentration	T (K)	Apparatus	Total CO_2 absorption capacity (mol CO_2/mol solution)	References
NaGly	10-30 wt%	303-323	Vapor-Liquid Equilibrium Cell	0.17-1.07	Song et. al (2006)
NaGly	1-30 wt%	298, 313	High Pressure Cell	0.5-1.6	Harris et. al (2009)
KGly	0.1-3 M	293-351	Stirred Reactor	0.1-1.4	Portugal et. al (2009)
KGly	0.1, 1, 3 M	308.15	N/A	0.456-2.62	Mohsin et. al (2018)
NaGly	0.1-1.5 M	293	Stirred Cell Reactor	0.09-0.20	This work
KGly	0.1-1.5 M	293	Stirred Cell Reactor	0.13-0.19	This work

Table 3. pH Measurements of Solutions Before and After CO2 Loading.

Solution	Molarity (M)	pH (Before CO_2-loading)	pH (After CO_2-loading)
KOH	0.1	12.50	12.45
	0.5	13.17	13.01
	1	13.39	13.29
	1.5	13.48	13.23
NaOH	0.1	12.95	12.56
	0.5	13.00	12.94
	1	13.05	12.90
	1.5	13.25	13.07
KGly	0.1	10.11	9.89
	0.5	10.25	10.12
	1	10.47	10.31
	1.5	10.60	10.47
NaGly	0.1	10.22	10.05
	0.5	10.54	10.49
	1	10.63	10.44
	1.5	10.77	10.32
Gly	0.1	6.23	5.90
	0.5	6.28	5.92
	1	6.33	5.95
	1.5	6.35	5.98

DOI: https://doi.org/10.22452/mjs.vol43sp1.10
Malaysian Journal of Science 43 (Special Issue 1): 58-66 (July 2024)

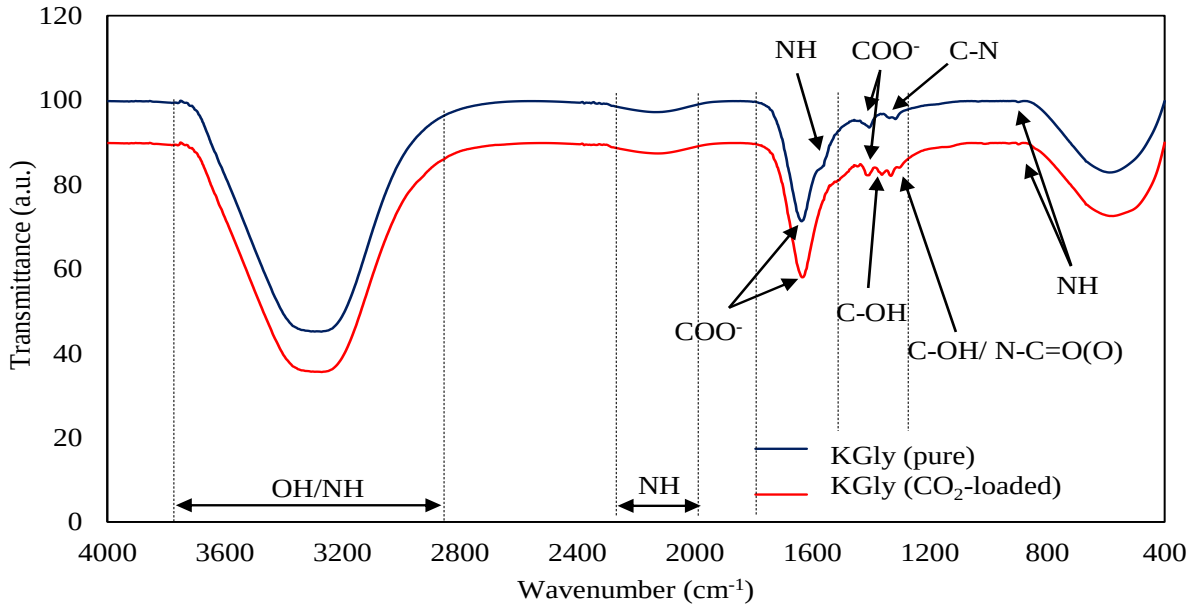

Figure 6. FTIR Spectra of KGly before and after CO_2 absorption.

approximately 1.4 times better results than sodium glycinate in terms of total CO_2 absorption capacity at the highest concentration.

According to Table 2, it can be said that sodium glycinate and potassium glycinate have different results under different experimental conditions. In this work, it was found that the experimental results of this work under atmospheric working conditions are lower than in the literature results. Studies can be carried out under higher pressure conditions and lower temperature conditions. Thus, higher absorption capacities can be achieved.

Table 3 shows the pH graph of the amino acid salt solutions potassium glycinate, sodium glycinate, and the alkaline solutions potassium hydroxide, sodium hydroxide before and after CO_2 loading. At high concentrations, the pH is also high due to the alkaline solution concentration. The high solution pH increases the reaction rate of CO_2 with OH^-. This causes an increase in the absorption rate of CO_2. At higher concentrations where the pH is high, the total CO_2 absorption capacity and dissolution rate experimental results are also better.

3.2. FTIR Results for Potassium Glycinate Solution

Potassium glycinate and sodium glycinate solutions have nearly similar results however, potassium glycinate gave slightly better results in terms of total CO_2 absorption capacity and dissolution rate. This comparison aroused the interest of the authors to observe the interaction between the amino acid salt solution and CO_2, and FTIR analysis was performed on pure and CO_2-loaded potassium glycinate solution for comparison. Functional groups of potassium glycinate were identified using Fourier Transform Infrared (FTIR) spectrometer (PerkinElmer) in METU Central Laboratory. FTIR spectra of potassium glycinate solution before and after CO_2 absorption were recorded at wavenumber ranging from 4000 to 400 cm^{-1} and results is shown in Fig. 6.

Fig. 6 shows that interactions occur between CO_2 and potassium glycinate due to the formation of new peaks as a result of CO_2-loaded. Table 4 indicates the characteristic peaks detected in the FTIR spectra of 0.5 M potassium glycinate solution before and after CO_2 absorption. While pure potassium glycinate FTIR spectrum is available in the literature, no data could be found for the CO_2-loaded potassium glycinate solution. Pure potassium glycinate FTIR spectra were also compared with Mohsin et al. (2018) and their results is also shown in Table 4.

Table 4. The Characteristics Peaks of Potassium Glycinate Before and After CO_2 Absorption.

Functional Groups	Wavenumber (cm^{-1}) This work Pure KGly	Wavenumber (cm^{-1}) This work CO_2-loaded KGly	Wavenumber (cm^{-1}) Mohsin et al. (2018) Pure KGly
OH/NH	3271	3270	3332
NH	2135	2126	2210
COO-	1636	1635	1630
NH	1559	-	1562
COO-	1405	1410	1404
C-OH	-	1362	-
C-OH/ N-C=O(O) (carbamate)	-	1332	-
C-N	1316	-	1320
NH	904	893	894

As can be seen in Table 4, the potassium glycinate spectrum was similar with the spectra reported by Mohsin et al. (2018). The OH characteristic peak was observed at approximately 3271 cm^{-1}, due to water molecules in KGly structure. The NH and COO^- peaks were observed 2135 and 1636 cm^{-1}, respectively. The last peaks

DOI: https://doi.org/10.22452/mjs.vol43sp1.10
Malaysian Journal of Science 43 (Special Issue 1): 58-66 (July 2024)

C-N and NH were observed at 1316 and 904 cm^{-1} and these peaks show the presence of amine in KGly structure. When the results of CO_2-loaded solution are examined, it can be seen that new peak intensities occur at 1332 and 1362 cm^{-1} wavenumbers. In the literature, the presence of C-OH functional groups in the range of 1400-1300 cm^{-1} and the presence of N-C=O(O) carbamate groups at 1322 cm^{-1} are mentioned (Jacson et al., 2009). The peaks here are thought to occur as a result of carbonate (CO_3^{2-}) and bicarbonate ions (HCO_3^-) formed as a result of the reaction of potassium glycinate solution with CO_2. Also in the literature, Falk & Miller (1992) reported peak intensities of 1385 cm^{-1} for CO_3^{2-} and 1360 cm^{-1} for HCO_3^-. According to the reaction mechanism between CO_2 and amino acid solution, carbamate and carbonate ions at similar peak intensities in the literature were determined by FTIR analysis in this study.

4. Conclusion

In this work, potassium and sodium glycinate solutions used as amino acid salt solutions were compared with alkaline solutions potassium and sodium hydroxide. The total CO_2 absorption capacity and dissolution rate of the solutions were investigated experimentally. According to the results, alkaline solutions gave the best results due to their high pH, while potassium glycinate gave approximately 1.4 times better results than sodium glycinate. In addition, characteristic functional groups were determined for both pure and CO_2-loaded solutions in FTIR analysis of potassium glycinate. According to the potassium glycinate-CO_2 reaction mechanism, it has been shown that carbamate and C-OH bonds are formed in the CO_2-loaded solution. When the study is evaluated, the use of amino acid salt solutions in CO_2 capture systems can reduce the use of toxic and hazardous solutions such as sodium hydroxide and potassium hydroxide, and also have the potential as promising solutions for CO_2 absorption. In the future, a detailed study of adding additives to amino acid salt solutions which will increase absorption performance, will be investigated.

5. Acknowledgement

The authors would like to acknowledge Em. Prof. Dr. Bekir Zühtü UYSAL for his valuable knowledge and constructive suggestions.

6. References

Aghel B., Maleki M., Sahraie S., & Heidaryan E. (2021). Desorption of carbon dioxide from a mixture of monoethanolamine with alcoholic solvents in a microreactor. *Fuel* 306:121636.

Ahn S., Song HJ., Park JW., Lee JH., Lee IY., & Jang KR. (2010). Characterization of metal corrosion by aqueous amino acid salts for the capture of CO_2. Korean J Chem Eng 27:1576-1580.

Ahmed R., Liu G., Yousaf B., Abbas Q., Ullah H., & Ali MU. (2020). Recent advances in carbon-based renewable adsorbent for selective carbon dioxide capture and separation-A review. *J Clean Prod* 242:118409.

Bernhardsen IM., & Knuutila HK. (2017). A review of potential amine solvents for CO_2 absorption process: absorption capacity, cyclic capacity and pKa. *Int J Grenh Gas Control* 61:27-48.

Buckingham J., Reina TR., & Duyar MS. (2022). Recent advances in carbon dioxide capture for process intensification, *Carbon Capture Science & Technology* 2:100031.

Babamohammadi S., Shamiri A., & Aroua MK. (2015). A review of CO_2 capture by absorption in ionic liquid-based solvents. *Rev Chem Eng* 31:383-412

Caplow, M. (1968) Kinetics of Carbamate Formation and Breakdown. *J. Am. Chem. Soc.* 90:6796.

Danckwerts, PV. (1979) The Reaction of CO_2 with Ethanolamines, *Chem. Eng. Sci*. 34:443.

Falk M., & Miller AG. (1992). Infrared spectrum of carbon dioxide in aqueous solution, *Vibrational Spectroscopy*, 4:105-108.

Fernandez ES., & Goetheer ELV. (2011). DECAB: process development of a phase change absorption process. *Energy Proceedia* 4:868-875.

Figueroa JD., Fout T., Plasynski S., McIlvried H., & Srivastava RD. (2008). Advances in CO_2 capture technology-The U.S. Department of Energy's Carbon Sequestration Program. *Int J Greenh. Gas Control* 2:9–20.

Gatti M., Martelli E., Marechal F., & Consonni S. (2014). Review, modeling, Heat Integration, and improved schemes of Rectisol®-based processes for CO_2 capture. *Appl. Therm. Eng.* 70:1123-1140.

Genç Çelikçi G. (2020). *Carbon Dioxide Capture in Structured Packing Column with n-Butanol and Ethyl Acetate*, Ph.D. Thesis, Gazi University, Ankara.

Ghosh UK., Kentish SE., & Stevens GW. (2009). Absorption of carbon dioxide into aqueous potassium carbonate promoted by boric acid. *Energy Procedia* 1:1075-1081.

Guo D., Thee H., Tan CY., Chen J., Fei W., Kentish SE., Stevens GW., & da Silva G. (2013). Amino Acids as Carbon Capture Solvents: Chemical Kinetics and Mechanism of the Glycine + CO_2 Reaction. *Energy &Fuels*, 27:3898-3904.

Harris F., Kurnia KA., Mutalib MI., & Thanapalan M. (2009). Solubilities of Carbon Dioxide and Densities of Aqueous Sodium Glycinate Solutions before and after CO_2 Absorption, *J. Chem. Eng. Data* 54:144-147.

Hu G., Smith KH., Wu Y., Mumford KA., Kentish SE., & Stevens GW. (2018). Carbon Dioxide Capture by Solvent Absorption Using Amino Acids: A Review. *Chin. J. Chem. Eng*. 26: 2229-2237.

IPCC. (2005). *Carbon Dioxide Capture and Storage*. Prepared by Working Group III of the Intergovernmental Panel on Climate Change, [Metz, B., O. Davidson, H. C. de Coninck, M. Loos, and L. A. Meyer (eds.)]. Cambridge University Press, Cambridge, UK and New York, NY, USA.

DOI: https://doi.org/10.22452/mjs.vol43sp1.10
Malaysian Journal of Science 43 (Special Issue 1): 58-66 (July 2024)

IPCC (2022). *Climate Change 2022: Impacts, Adaptation and Vulnerability.* Contribution of Working Group II to the Sixth Assessment Report of the Intergovernmental Panel on Climate Change [H.-O. Pörtner, D.C. Roberts, M. Tignor, E.S. Poloczanska, K. Mintenbeck, A. Alegría, M. Craig, S. Langsdorf, S. Löschke, V. Möller, A. Okem, B. Rama (eds.)]. Cambridge University Press. Cambridge University Press, Cambridge, UK and New York, NY, USA.

Jacson P., Robinson K., Puxty G., & Attalla M. (2009). In situ Fourier Transform-Infrared (FT-IR) analysis of carbon dioxide absorption and desorption in amine solution, *Energy Procedia*, 1:985-994.

Keith DW., Holmes G., St. Angelo D., & Heidel K. (2018). A process for capturing CO_2 from the atmosphere. *Joule* 2:1573-1594.

Kucka L., Richter J., Kenig EY., & Górak A. (2003). Determination of gas–liquid reaction kinetics with a stirred cell reactor. *Sep. Purif. Technol*. 2:163-175.

Kumar PS., Hongendoorn JA., Versteeg GF., & Veron PHM. (2003). Kinetics of the Reaction of CO_2 with Aqueous Potassium Salt of Taurine and Glycine. *AIChE J*. 49: 203-213.

Lee S., Song H., Maken S., & Park J. (2007). Kinetics of CO_2 Absorption in Aqueous Sodium Glycinate Solutions, *Ind. Eng. Chem. Res*. 46: 1578-1583.

Li J., Ye Y., Chen L., & Qi Z. (2012). Solubilities of CO_2 in Poly(ethylene glycols) from (303.15 to 333.15) K. *J. Chem. Eng. Data* 57:610-616.

Luis P. (2016). Use of monoethanolamine (MEA) for CO_2 capture in a global scenario: Consequences and alternatives. *Desalination* 380:93-99.

Majchrowicz ME., Kersten S., & Brilman W. (2014). Reactive Absorption of Carbon Dioxide in L-Prolinate Salt Solutions. *Ind. Eng. Chem. Res.* 53:11460-11467.

Mohsin HM., Johari K., & Shariff AM. (2018). Virgin coconut oil (VCO) and potassium glycinate (PG) mixture as absorbent for carbon dioxide capture, *Fuel* 232:454-462.

Murrieta-Guevara F., Romero-Martinez A., & Trejo A. (1988). Gas solubilities of carbon dioxide and hydrogen sulfide in sulfolane and its mixtures with alkanolamines. *Fluid Ph. Equilibria* 44:105-115.

National Aeronautics and Space Administration (NASA), Climate Change Carbon Dioxide Latest Measurements, United States https://climate.nasa.gov/vital-signs/carbon-dioxide/ (accessed 2023-06-22).

Ochedi FO., Yu J., Yu H., Liu Y., & Hussain A. (2021). Carbon dioxide capture using liquid absorption methods: a review, Environmental *Chemistry Letters*, 19:77-109.

Olajire AA. (2010) CO_2 capture and separation technologies for end-of-pipe applications–A review. *Energy* 35:2610-2628.

Portugal A., Sousa J., Magalhães F., & Mendes A. (2009). Solubility of carbon dioxide in aqueous solutions of amino acid salts. *Chem. Eng. Sci.* 64: 1993–2002.

Puxty G., Rowland R., Allport A., Yang Q., Bown M., Burns R., & Attala M. (2009). Carbon Dioxide Postcombustion Capture: A Novel Screening Study of The Carbon Dioxide Absorption Performance of 76 Amines. *Environ. Sci. Technol.* 43:6427-6433.

Smith JM., Van Ness HC., Abbott MM., & Swihart MT. (2022) *Introduction to Chemical Engineering Thermodynamics*, pp. 78, New York, USA: Mc Graw-Hill.

Song H., Lee S., Maken S., Park JJ., & Park JW. (2006). Solubilities of carbon dioxide in aqueous solutions of sodium glycinate. *Fluid Phase Equil*. 246: 1–5.

Thee H., Nicholas J., Smith KH., da Silva G., Kentish SE., & Stevens GW. (2013). A kinetic study of CO_2 capture with potassium carbonate solutions promoted with various amino acids: Glycine, sarcosine and proline. *Int. J. Greenh. Gas Control.* 20:212-222.

Uysal D. (2016). *Absorption of Carbon Dioxide into Calcium Acetate Solution*, Ph.D. Thesis, Gazi University, Ankara.

Vaidya PD., Konduru P., Vaidyanathan M., & Kenig EY. (2010). Kinetics of carbondioxide removal by aqueous alkaline amino acid salts. *Ind. Eng. Chem. Res.* 49:11067–11072.

Wang F., Zhao J., Miao H., Zhao J., Zhang H., Yuan J., & Yan J. (2018). Current status and challenges of the ammonia escape inhibition technologies in ammonia-based CO_2 capture technologies, *Appl. Energy* 230:734-749.

Wang M., Lawal A., Stephenson P., Sidders J., & Ramshaw C. (2011). Post-combustion CO_2 capture with chemical absorption: a state-of-the-art-review. *Chem. Eng. Res. Des.* 89:1609-1624.

Wu Y., Xu J., Mumford K., Stevens GW., Fei W., & Wang Y. (2020). Recent advances in carbon dioxide capture and utilization with amines and ionic liquids. *Green. Chem. Eng.* 1:16-32.

Ying J., & Eimer DA. (2013). Determination and measurements of mass transfer kinetics of CO_2 in concentrated aqueous monoethanolamine solutions by a stirred cell *Ind. Eng. Chem. Res*. 52: 2548–2559.

Yuan X., Wang J., Deng S., Suvarna M., Wang X., Zhang W., Hamilton ST., Alahmed A., Jamal A., Park AHA., Bi X., & Ok YS. (2022). Recent advancements in sustainable upcycling of solid waste into porous carbons for carbon dioxide capture. *Renewable Sustainable Energy Rev.* 162:112413.

Zhang Z., & Huisingh D. (2017). Carbon dioxide storage schemes: technology, assessment and deployment. *J. Clean. Prod.* 142:1055-1064.

DOI: https://doi.org/10.22452/mjs.vol43sp1.10
Malaysian Journal of Science 43 (Special Issue 1): 58-66 (July 2024)